

## Elastic Scattering of $\pi^\pm$ -Mesons on ${}^4\text{He}$ in the Energy Interval (68÷208) MeV.

YU. A. SHCHERBAKOV, T. ANGELESCU, I. V. FALOMKIN, M. M. KULYUKIN  
V. I. LYASHENKO, R. MACH, A. MIHUL, N. M. KAO, F. NICHITIU  
G. B. PONTECORVO, V. K. SARYCHIEVA, M. G. SAPOZHNIKOV  
M. SEMERDJIEVA, T. M. TROSHEV and N. I. TROSHEVA

*Joint Institute for Nuclear Research - Dubna*

F. BALESTRA, L. BUSSO, R. GARFAGNINI and G. PIRAGINO

*Istituto di Fisica dell'Università - Torino*

*Istituto Nazionale di Fisica Nucleare - Sezione di Torino*

(ricevuto l'8 Settembre 1975)

**Summary.** — Differential cross-section measurements of elastic scattering of  $\pi^\pm$  on  ${}^4\text{He}$  are presented. The experiment was carried out with the high-pressure helium self-shunted streamer chamber surrounded by a hodoscope of scintillation counters. Measurements were fulfilled both for positive and negative pions at 68, 98, 135, 145 and 156 MeV, for negative pions also at 120, 174 and 208 MeV. The differential and total elastic-scattering cross-sections are compared with optical-model calculations using the Kisslinger and Laplacian potentials. Some results, obtained from an energy-dependent phase shift analysis, are also presented.

### I. - Introduction.

First results of our experiment on elastic scattering of pions on  ${}^4\text{He}$ , carried out at the Laboratory of Nuclear Problems of the JINR, have been described in ref. (1,2). The experiment was performed using a high-pressure helium self-

---

(1) I. V. FALOMKIN, M. M. KULYUKIN, V. I. LYASHENKO, F. NICHITIU, G. B. PONTECORVO, G. PIRAGINO and YU. A. SHCHERBAKOV: *Lett. Nuovo Cimento*, **3**, 461 (1972); **5**, 1121 (1972).

(2) I. V. FALOMKIN, M. M. KULYUKIN, V. I. LYASHENKO, G. B. PONTECORVO, YU. A. SHCHERBAKOV, M. ALBU, T. BESLIU, A. MIHUL, F. NICHITIU, R. GARFAGNINI and G. PIRAGINO: *Nuovo Cimento*, **21 A**, 168 (1974).

TABLE I. --  $(\pi^\pm, {}^4\text{He})$  elastic-scattering differential cross-sections at 98, 135, 145, 156 MeV and  $(\pi^-, {}^4\text{He})$  at 120, 174, 208 MeV.

98 MeV				
$\theta_{\text{c.m.}}$	$(\pi^+, {}^4\text{He})$		$(\pi^-, {}^4\text{He})$	
	$d\sigma/d\Omega$ (mb/sr)	$\varepsilon$ (mb/sr)	$d\sigma/d\Omega$ (mb/sr)	$\varepsilon$ (mb/sr)
31.8	12.70	0.99	15.42	0.87
42.2	8.76	0.65	10.72	0.59
52.7	4.65	0.41	4.92	0.34
63.0	2.17	0.27	1.96	0.20
73.3	0.60	0.14	0.96	0.16
83.4	0.76	0.17	1.39	0.18
93.5	2.19	0.27	0.84	0.17
103.4	2.90	0.32	2.28	0.23
113.2	3.52	0.35	3.06	0.27
123.0	3.47	0.34	4.21	0.28
132.6	4.50	0.39	4.25	0.30
142.2	5.07	0.43	4.70	0.32
151.7	4.40	0.39	3.96	0.29
161.1	4.39	0.40	4.17	0.32
120 MeV				
$\theta_{\text{c.m.}}$	$(\pi^-, {}^4\text{He})$			
	$d\sigma/d\Omega$ (mb/sr)	$\varepsilon$ (mb/sr)		
29.3	36.36	5.85		
34.6	32.37	4.27		
39.9	24.48	3.18		
45.1	12.42	2.03		
50.4	10.23	1.74		
58.1	4.76	0.81		
76.1	0.88	0.22		
96.3	2.25	0.48		
111.1	3.68	0.62		
123.2	4.77	0.88		
132.9	3.67	0.77		
142.4	4.73	0.90		
151.9	4.61	0.90		
163.6	3.04	0.64		

TABLE I (continued).

135 MeV				
$\theta_{\text{c.m.}}$	$(\pi^+, {}^4\text{He})$		$(\pi^-, {}^4\text{He})$	
	$d\sigma/d\Omega$ (mb/sr)	$\varepsilon$ (mb/sr)	$d\sigma/d\Omega$ (mb/sr)	$\varepsilon$ (mb/sr)
29.4	43.17	3.93	50.23	5.65
34.7	31.98	2.66	35.84	3.57
40.0	23.76	2.01	24.82	2.59
45.3	16.76	1.50	14.66	1.74
50.5	7.15	0.91	7.69	1.71
55.7	4.55	0.71	5.77	0.97
60.9	2.87	0.57	2.65	0.65
68.7	1.19	0.26	1.37	0.32
78.9	0.94	0.23	1.05	0.28
89.0	1.10	0.25	1.40	0.34
99.0	1.60	0.30	1.66	0.38
108.8	3.13	0.42	1.78	0.37
118.6	2.34	0.37	2.72	0.48
128.2	2.77	0.41	1.96	0.42
137.8	1.92	0.33	1.72	0.39
147.2	2.13	0.36	0.94	0.28
156.6	1.52	0.30	1.06	0.31
166.0	1.88	0.44	1.47	0.46

145 MeV				
$\theta_{\text{c.m.}}$	$(\pi^+, {}^4\text{He})$		$(\pi^-, {}^4\text{He})$	
	$d\sigma/d\Omega$ (mb/sr)	$\varepsilon$ (mb/sr)	$d\sigma/d\Omega$ (mb/sr)	$\varepsilon$ (mb/sr)
29.5	48.54	4.76	38.46	3.23
34.8	39.41	3.53	28.55	2.25
40.1	25.46	2.51	22.11	1.76
45.4	17.73	1.93	13.24	1.24
50.6	4.24	0.89	5.68	0.80
55.8			2.95	0.56
58.4	2.13	0.44		
63.6			2.62	0.36
71.3	0.98	0.24		
76.4			1.68	0.25
86.6	1.21	0.27		
89.1			2.34	0.36
99.1	2.75	0.51	2.26	0.35
109.0	1.80	0.41	2.01	0.33
118.7	2.17	0.45		
121.1			1.62	0.24
130.7	2.18	0.36		
135.5			1.57	0.23
144.9	1.35	0.28		
149.7			0.98	0.18
161.4	1.26	0.29		
163.7			0.87	0.21

TABLE I (continued).

156 MeV				
$\theta_{c.m.}$	$(\pi^+, {}^4\text{He})$		$(\pi^-, {}^4\text{He})$	
	$d\sigma/d\Omega$ (mb/sr)	$\varepsilon$ (mb/sr)	$d\sigma/d\Omega$ (mb/sr)	$\varepsilon$ (mb/sr)
29.5	52.91	4.07		
34.9	42.70	2.84	32.33	2.75
40.2	26.86	2.03	27.14	2.21
45.5	15.60	1.44	14.29	1.41
50.7	7.70	0.98	8.40	1.02
56.0	5.58	0.82	5.49	0.77
66.3	2.19	0.29	1.95	0.25
81.7	1.09	0.21	1.19	0.19
96.7	1.48	0.23	1.90	0.24
111.5	1.94	0.28	1.63	0.22
126.0	1.52	0.24	0.89	0.16
140.3	1.19	0.21	0.68	0.14
156.7	0.75	0.15	0.39	0.10

174 MeV			208 MeV		
$\theta_{c.m.}$	$(\pi^-, {}^4\text{He})$		$\theta_{c.m.}$	$(\pi^-, {}^4\text{He})$	
	$d\sigma/d\Omega$ (mb/sr)	$\varepsilon$ (mb/sr)		$d\sigma/d\Omega$ (mb/sr)	$\varepsilon$ (mb/sr)
29.6	41.26	5.16	20.9	30.50	2.95
35.0	28.62	3.22	35.2	24.93	2.13
40.3	20.29	2.33	40.6	18.91	1.63
48.3	9.80	0.99	45.9	9.15	1.00
56.2	3.04	0.74	51.2	3.58	0.57
61.4	1.79	0.56	56.5	1.83	0.40
74.2	0.60	0.17	64.4	0.44	0.14
92.0	0.70	0.22	79.8	0.21	0.07
106.8	0.75	0.22	94.9	0.46	0.15
123.8	0.36	0.14	109.7	0.25	0.08
140.5	0.40	0.16	126.6	0.22	0.09
159.1	0.22	0.11	140.7	0.27	0.10
			159.3	0.16	0.06

shunted streamer chamber surrounded by a scintillation counter hodoscope <sup>(1)</sup> covering the angular interval ( $25^\circ \div 165^\circ$ ).

The central beam energy values were determined with an accuracy of ( $2 \div 3$ ) MeV and the energy spread was of ( $4 \div 8$ )%. The percentage of pions in the beam varied from 60% up to 95% depending on the pion energy and on the pion charge sign. The beam contamination was measured with a total energy loss Čerenkov counter with an accuracy better than 3%. In the present work improved data with higher statistics are given at the old energies <sup>(1,2)</sup>, and new measurements of differential cross-sections at 120, 135, 145, 156, 174 and 208 MeV are presented.

## 2. - Results.

In Table I the differential elastic-scattering cross-sections are presented as functions of the angles in the centre-of-mass system. The quoted errors are statistical only. At 174 and 208 MeV the measurements were carried out only with  $\pi^-$  because at these energies there were not available  $\pi^+$  beams of sufficient intensity. The data we obtained at 68 MeV with negative and positive pions are not included in the Table I because they were presented in ref. <sup>(2)</sup>.

TABLE II.

$T_\pi$ (MeV)	$(\pi^-, {}^4\text{He})$		$(\pi^+, {}^4\text{He})$	
	$\sigma_{el}$ (mb)	Number of events	$\sigma_{el}$ (mb)	Number of events
68	$36 \pm 3$	779	$35 \pm 3$	606
98	$62 \pm 6$	2354	$60 \pm 6$	1447
120	$99 \pm 6$	464		
135	$114 \pm 7$	636	$106 \pm 7$	999
145	$102 \pm 6$	1012	$110 \pm 8$	648
156	$94 \pm 7$	797	$117 \pm 8$	971
174	$90 \pm 7$	396		
208	$80 \pm 8$	584		

Table II shows  $(\pi^\pm, {}^4\text{He})$  elastic-scattering total cross-sections for different energies and also the total number of measured (in the experimental angular interval) events for each energy. The values of the cross-sections were evaluated by integrating best-fit curves fitted to the experimental values of the differential

cross-sections <sup>(3)</sup>. The total cross-section values are given from 0° to 180° and the quoted errors are not only statistical but the possible uncertainty due to the integration procedure was taken into account.

### 3. - Discussion of the results.

The experimental angular distributions were compared with optical-model calculations as in ref. <sup>(4,5)</sup>. In these calculations the impulse and also the coherent scattering approximations were used and the Fermi motion of the nucleons in the nucleus and the recoil of the nucleus itself were taken into account.

Two potentials were used, the Kisslinger potential

$$(1) \quad \langle \mathbf{r} | V_{\mathbf{K}} \psi \rangle = 2\mathcal{M}V_c(r)\psi(\mathbf{r}) + (A-1) \cdot \\ \cdot \left\{ B\varrho(r)\psi(\mathbf{r}) + C \left[ -\nabla(\varrho(r)\nabla\psi(\mathbf{r})) + \frac{A-1}{A} \frac{\mathcal{M}}{2M} (\nabla^2\varrho(r)\psi(\mathbf{r})) \right] \right\},$$

and the Laplacian potential

$$(2) \quad \langle \mathbf{r} | V_{\mathbf{L}} \psi \rangle = 2\mathcal{M}V_c(r)\psi(\mathbf{r}) + \\ + (A-1) \left\{ (B + p_{\text{ACM}}^2 C)\varrho(r) + \frac{1}{2} \frac{\mathcal{M}^2}{\mu^2} C(\nabla^2\varrho(r)) \right\} \psi(\mathbf{r}).$$

Here  $B = -(4\pi/p_{\text{ACM}})(\mathcal{M}^2/\mu^2)b$  and  $C = -(4\pi/p_{\text{ACM}}^3)(\mathcal{M}^2/\mu^2)c$ .

In these expressions  $p_{\text{ACM}}$  is the pion momentum of the pion-<sup>4</sup>He system. The coefficients  $b$  and  $c$  were deduced from the analysis of AUERBACH *et al.* <sup>(6)</sup> using the phase shifts given in ref. <sup>(7)</sup>.  $\mathcal{M}$  and  $\mu$  are the reduced masses of the pion-nucleus and pion-nucleon system respectively. The total collision energy  $E$  in the pion-nucleus c.m. system was

$$E = (p_{\text{ACM}}^2 + m^2)^{\frac{1}{2}} + (p_{\text{ACM}}^2 + A^2 M^2)^{\frac{1}{2}},$$

where  $m$  is the pion mass,  $M$  is the mass of the nucleon and  $A$  is the number of nucleons in the nucleus.

<sup>(3)</sup> I. V. FALOMKIN, M. M. KULYUKIN, V. I. LYASHENKO, A. MIHUL, F. NICHITU, G. PIRAGINO, G. B. PONTECORVO and YU. A. SHCHERBAKOV: preprint JINR, E1-6534, Dubna (1972).

<sup>(4)</sup> R. MACH: *Nucl. Phys.*, **205** A, 56 (1973).

<sup>(5)</sup> R. MACH: *Phys. Lett.*, **40** B, 46 (1972).

<sup>(6)</sup> E. H. AUERBACH, D. M. FLEMING and M. M. STERNHEIM: *Phys. Rev.*, **162**, 1683 (1967).

<sup>(7)</sup> S. ALMEHED and C. LOVELACE: *Nucl. Phys.*, **40** B, 157 (1972).

In the expressions (1) and (2)  $V_c(r)$  is the Coulomb potential, and  $\rho(r)$  is the density distribution of nuclear matter, which was supposed to be

$$(3) \quad \rho(r) = \frac{1}{(a^2\pi)^{\frac{3}{2}}} \exp\left[-\frac{r^2}{a^2}\right].$$

The parameter  $a$  was determined using the charge radius  $R_{\text{He}} = 1.71$  fm, as experimentally deduced by FRESH *et al.* <sup>(8)</sup>, and the proton radius  $r_p = 0.8$  fm. The parameter  $a$  is connected in the following way to the values  $r_p$  and  $R_{\text{He}}$ :

$$a^2 = \frac{2}{3} (R_{\text{He}}^2 - r_p^2).$$

The pion- ${}^4\text{He}$  scattering phase shifts were obtained by «matching» the

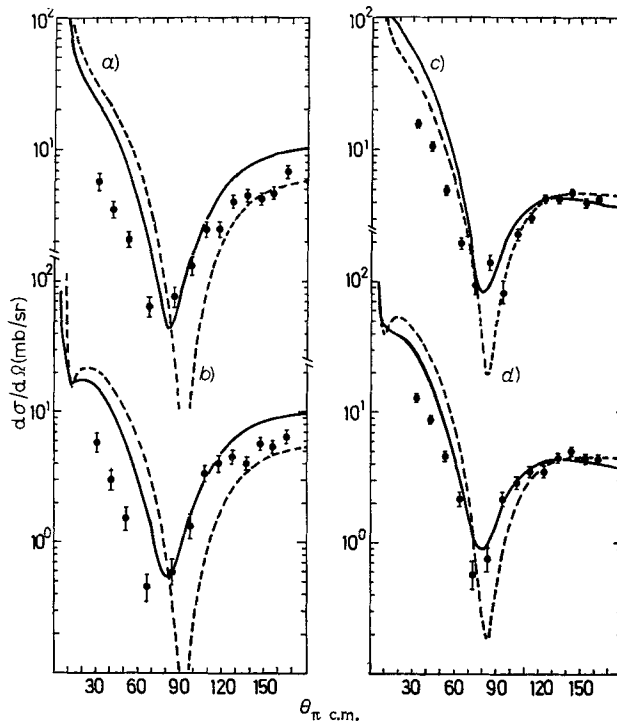


Fig. 1. —  $(\pi^\pm, {}^4\text{He})$  elastic-scattering differential cross-sections at 68 and 98 MeV. The curves are obtained from optical-model calculations using the Kisslinger (full line) and the Laplacian (dashed line) potentials. a)  $(\pi^-, {}^4\text{He})$  68 MeV, b)  $(\pi^+, {}^4\text{He})$  68 MeV, c)  $(\pi^-, {}^4\text{He})$  98 MeV, d)  $(\pi^+, {}^4\text{He})$  98 MeV.

<sup>(8)</sup> R. F. FRESH, J. S. MC CARTHY, R. E. REND and M. R. YARIAN: *Phys. Rev.*, **160**, 874 (1967).

solutions of the Schrödinger equation, solved with potentials (1) and (2), and the Coulomb wave functions outside nuclear-force region. A detailed description of this procedure is given in ref. (9) where first experimental data were analysed.

Figures 1, 2 and 3 present the experimental values of the differential cross-sections for different energies, and also the results obtained from optical-model calculations with the Kisslinger and Laplacian potentials. The results obtained using the Kisslinger potential seem to be in better agreement with experimental data (although in the region of small angles the theoretical values are considerably higher than the experimental ones obtained using the two potentials considered), in particular in the region of the first minimum. At

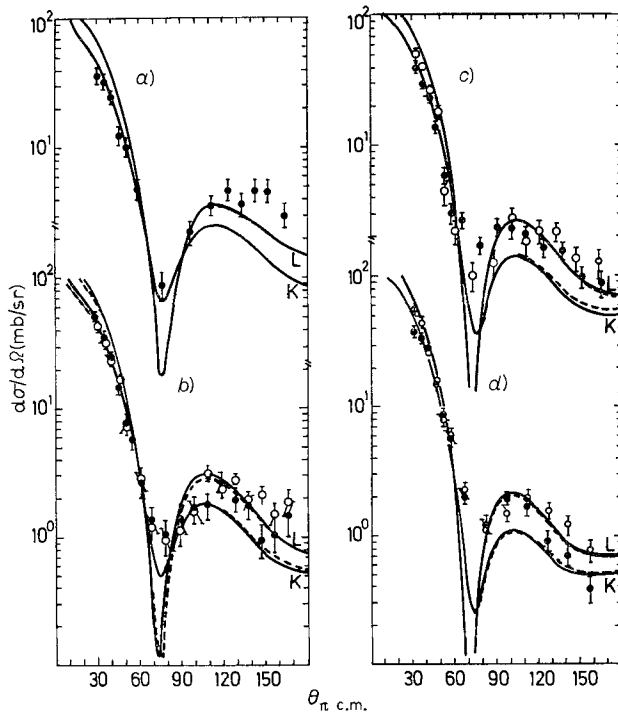


Fig. 2. — ( $\pi^-$ ,  ${}^4\text{He}$ ) elastic-scattering differential cross-section at 120, 135, 145, 156 MeV (full points). ( $\pi^+$ ,  ${}^4\text{He}$ ) at 135, 145, 156 MeV (open circles). The curves are obtained from optical-model calculations using Kisslinger (curve K) and Laplacian (curve L potentials). The full lines are for  $\pi^-$ -mesons and the dashed lines are for  $\pi^+$ -mesons. a) ( $\pi^-$ ,  ${}^4\text{He}$ ) 120 MeV, b) ( $\pi^\pm$ ,  ${}^4\text{He}$ ) 135 MeV, c) ( $\pi^\pm$ ,  ${}^4\text{He}$ ) 145 MeV, d) ( $\pi^\pm$ ,  ${}^4\text{He}$ ) 156 MeV.

(9) L. ALEKSANDROV, T. ANGELESCU, I. V. FALOMKIN, F. NICHITU and YU. A. SHCHERBAKOV: preprint JINR, P1-8328, Dubna (1974).



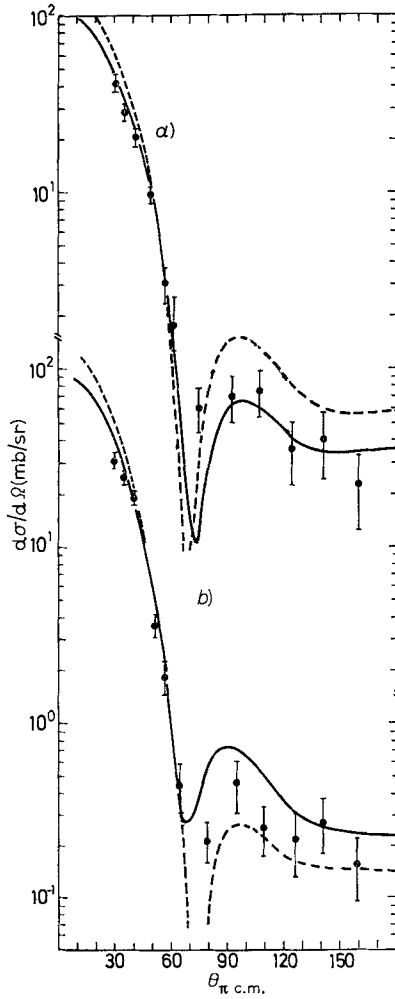


Fig. 3. - ( $\pi^-$ ,  ${}^4\text{He}$ ) elastic-scattering differential cross-sections at *a*) 174 and *b*) 208 MeV. The curves are obtained from optical-model calculations using Kisslinger (full line) and Laplacian (dashed line) potentials.

large angles the statistics is not sufficient to discriminate between the two potentials we used.

Figure 4 shows the energy behaviour of the ( $\pi^\pm$ ,  ${}^4\text{He}$ ) elastic-scattering total cross-sections. In the same Figure the results of calculations with the Laplacian and Kisslinger potentials are also presented for the ( $\pi^-$ ,  ${}^4\text{He}$ ).

The values obtained with the Kisslinger potential are in better agreement with experiment, although at energies lower than 100 MeV they are greatly higher than experimental data. In the case of the ( $\pi^-$ ,  ${}^4\text{He}$ ) elastic scattering the total cross-section presents a maximum value at about 150 MeV.

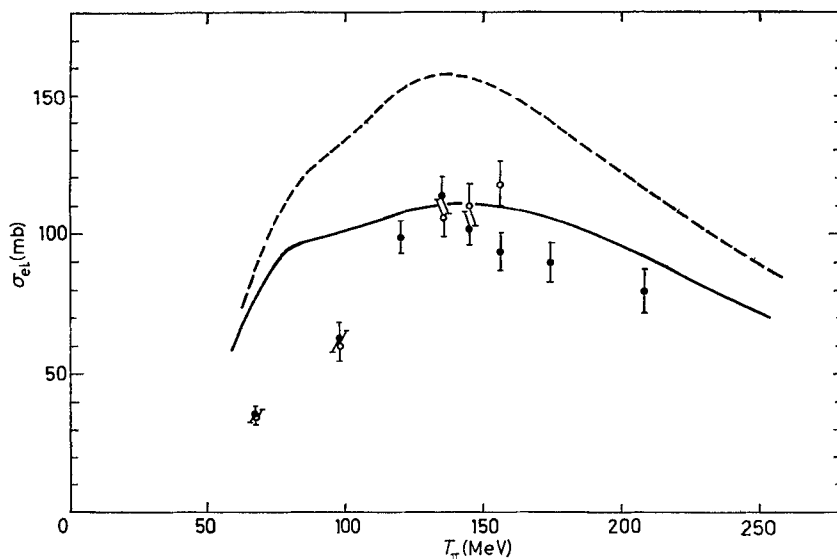


Fig. 4. — Total cross-sections for  $(\pi^\pm, {}^4\text{He})$  elastic scattering as a function of the pion kinetic energy:  $\bullet$  ( $\pi^-, {}^4\text{He}$ );  $\circ$  ( $\pi^+, {}^4\text{He}$ ). The curves are obtained from optical-model calculations with Kisslinger (full line) and Laplacian (dashed line) potentials.

The small angle discrepancies between calculated and measured results observed at energies lower than 100 MeV can be probably ascribed to the fact that the coherent scattering approximation is no longer valid in this energy region.

The influence of the intermediate nuclear excitation on the elastic scattering (or equivalently, corrections to the coherent scattering approximation) can be roughly estimated utilizing the modified Kisslinger potential as suggested in ref. (10). At low energies this modification leads to a noticeable decrease of the differential cross-sections at small angles. As it will be discussed below, the energy dependent  $\pi$ - ${}^4\text{He}$  phase-shift analysis provides an additional qualitative indication upon the excited intermediate states contribution to the elastic scattering. Using all existing data on the differential and total elastic cross-sections an energy-dependent phase shift analysis (9) has been performed. The following parametrization (see ref. (11)) for the phase shifts was used:

$$k^{2l+1} \text{ctg } \Delta_l = \frac{1}{a_l} + b_l T + c_l T^2 + \dots,$$

where  $T$  is the kinetic energy in the laboratory system,  $a_l$ ,  $b_l$ ,  $c_l$  are complex

(10) M. ERICSON and T. E. O. ERICSON: *Ann. of Phys.*, **36**, 323 (1966).

(11) R. A. ARNDT, D. D. LONG and L. D. ROEPER: *Nucl. Phys.*, **209 A**, 429, 447 (1973).

values and  $\Delta_l$  is the corresponding partial phase. The coefficient  $a_l$  is the scattering length.

In fig. 5 Argand diagrams for three partial waves ( $l = 2, 1, 0$ ) are shown. These diagrams are deduced using experimental data and also the phase shifts calculated on base of the optical model with the Laplacian and Kisslinger poten-

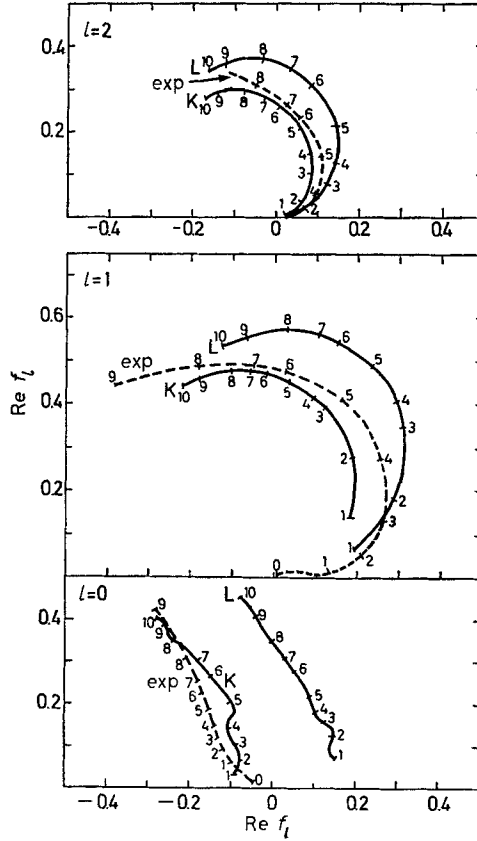


Fig. 5. — Argand plots for three partial waves for  $l = 0, 1, 2$ . The plots are obtained from an energy-dependent phase shift analysis of the elastic scattering of pions on  ${}^4\text{He}$  (dashed line). The K and L curves are obtained from optical-model calculations with Kisslinger and Laplacian potentials respectively. The table shows the correspondence between the points and the pion energy.

$n$	$T_\pi$ (MeV)	$n$	$T_\pi$ (MeV)
0	10	6	140
1	50	7	150
2	70	8	170
3	90	9	200
4	100	10	220
5	120		

tials. In the case of the  $S$ -wave the Kisslinger potential is in better agreement with experimental data, but in the case of  $P$  and  $D$  waves it is more difficult to discriminate between the two potentials.

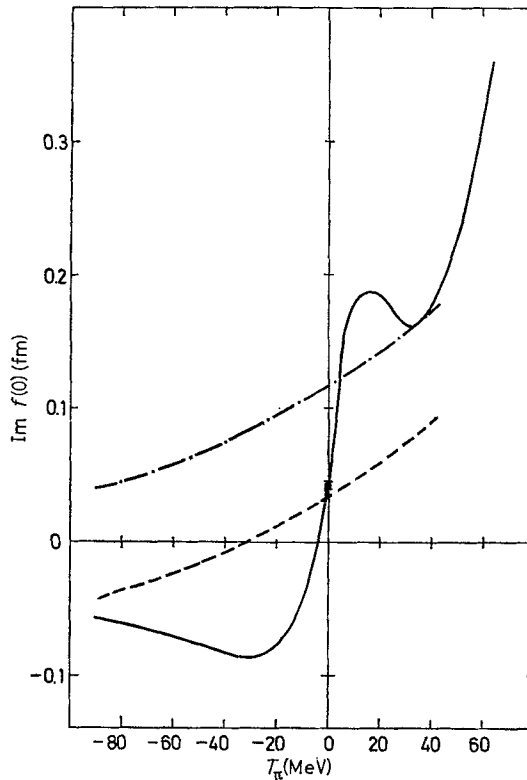


Fig. 6. — Imaginary part of the «forward» amplitude for elastic scattering of pions on  ${}^4\text{He}$  as a function of the pion energy (in the physical and nonphysical regions): full line, from an energy-dependent phase shift analysis<sup>(9)</sup>; dot-dashed line, from ref. (12); dashed line, from ref. (13). The experimental point at  $T=0$  is obtained from experiments with mesoatoms<sup>(11)</sup>.

Figure 6 shows the behaviour of the imaginary part of «forward» amplitude  $\text{Im } f(0)$  obtained with the energy-dependent phase shift analysis. As one can see, in the nonphysical region the behaviour of the imaginary part differs from that obtained in ref. (12,13) using forward dispersion relations in the analysis of pion-nucleus scattering. The imaginary part of the scattering length is in good agreement with the values obtained from helium mesoatom

(12) T. E. O. ERICSON and M. P. LOCHER: *Nucl. Phys.*, **148** A, 1 (1970).

(13) C. J. BATTY, G. T. A. SQUIER and G. K. TURNER: *Nucl. Phys.*, **67** B, 492 (1973).

experiments<sup>(14)</sup>. In our case the scattering lengths turn out to be  $\text{Re } a_0 = 0.160 \pm 0.010$  and  $\text{Im } a_0 = 0.055 \pm 0.007$  (\*). Moreover, the  $\text{Im } f(0)$  values show an enhancement in the energy interval, in which the low lying  ${}^4\text{He}$  excited states are located ( $\sim 20$  MeV). The  $P$ -wave phase-shift exhibits corresponding structure in the same energy region (9). The enhancement shown in fig. 6 seems to indicate that some information on nuclear excited states is contained in the elastic differential and total cross-sections measured even at present level of accuracy. The target nucleus plays probably less inert role than that assumed in constructing the existing optical potentials.

\* \* \*

The authors are grateful to V. P. DZHELEPOV and L. J. LAPIDUS for their continuous encouragement and support, to V. B. BELIYAIEV, V. C. LUKYANOV and R. A. ERAMZHAN for the helpful discussions. They are very grateful to the synchrocyclotron staff and to the staff of the electronic department for the essential assistance throughout the experiment.

---

<sup>(14)</sup> G. BACHENSTOSS, I. BERGSTRÖM, J. EGGER, R. HAGELBERG, C. J. HERRLANDER, H. KOCH, H. P. POVEL, R. H. PRICE, A. SCHWITTER and L. TAUSHER: *Nucl. Phys.*, **66** B, 125 (1973); IL-TONG CHEON and T. VON EGIDY: preprint, Institute de Physique Université de Liège, Belgium (1974).

(\*) One of the parameters in the phase shift analysis (9) is the electromagnetic radius of the pion. If we use the method described in ref. (15) from our analysis the radius results  $\langle r^2 \rangle^{\frac{1}{2}} = (0.83 \pm 0.17)$  fm.

<sup>(15)</sup> F. NICHITIU and YU. A. SHCHERBAKOV: *Nucl. Phys.*, **61** B, 429 (1973).

## ● RIASSUNTO

Sono presentati i risultati della misura della sezione d'urto differenziale di diffusione elastica ( $\pi^\pm, {}^4\text{He}$ ) a 68, 98, 135, 145, 156 MeV e ( $\pi^-, {}^4\text{He}$ ) a 120, 174, 208 MeV. I dati sperimentali sono confrontati con le previsioni del modello ottico. È stata pure fatta un'analisi in fase dipendente dell'energia.

**Рассеяние заряженных пионов на ядрах  ${}^4\text{He}$  в диапазоне энергий (68 ÷ 208) МэВ.**

**Резюме.** — Приводятся новые данные по дифференциальным сечениям упругого рассеяния заряженных пионов на ядрах гелия-4, полученные в экспериментах с гелиевой струйной камерой высокого давления на синхротронном ЛЯП ОИЯИ. Приводятся данные по фазовому анализу, зависящему от энергии, проводится сравнение с расчетами по оптической модели.